

pubs.acs.org/joc Featured Article

# Deciphering Reactivity and Selectivity Patterns in Aliphatic C-H Bond Oxygenation of Cyclopentane and Cyclohexane Derivatives

Teo Martin, <sup>⊥</sup> Marco Galeotti, <sup>⊥</sup> Michela Salamone, Fengjiao Liu, \* Yanmin Yu, Meng Duan, K. N. Houk, \* and Massimo Bietti \*



Cite This: J. Org. Chem. 2021, 86, 9925–9937



**ACCESS** 

III Metrics & More

Article Recommendations

s Supporting Information

**ABSTRACT:** A kinetic, product, and computational study on the reactions of the cumyloxyl radical with monosubstituted cyclopentanes and cyclohexanes has been carried out. HAT rates, site-selectivities for C–H bond oxidation, and DFT computations provide quantitative information and theoretical models to explain the observed patterns. Cyclopentanes functionalize predominantly at C-1, and tertiary C–H bond activation barriers decrease on going from methyl- and *tert*-butylcyclopentane to phenylcyclopentane, in line with the computed C–H BDEs. With cyclohexanes, the relative importance of HAT from C-1 decreases on going from methyl- and phenylcyclohexane to ethyl-, isopropyl-, and *tert*-butylcyclohexane. Deactivation is also observed at C-2 with site-selectivity that progressively shifts to C-3 and C-4 with increasing

substituent steric bulk. The site-selectivities observed in the corresponding oxidations promoted by ethyl(trifluoromethyl)dioxirane support this mechanistic picture. Comparison of these results with those obtained previously for C–H bond azidation and functionalizations promoted by the PINO radical of phenyl and *tert*-butylcyclohexane, together with new calculations, provides a mechanistic framework for understanding C–H bond functionalization of cycloalkanes. The nature of the HAT reagent, C–H bond strengths, and torsional effects are important determinants of site-selectivity, with the latter effects that play a major role in the reactions of oxygen-centered HAT reagents with monosubstituted cyclohexanes.

## **■ INTRODUCTION**

Aliphatic C–H bond functionalization is now a well-accepted method of late-stage functionalization. The direct introduction of a variety of functional groups in place of H is currently one the most investigated approaches to new synthetic methodology. Radical substitution processes are perhaps the oldest known methods for aliphatic C–H functionalization. However, because of the multitude of C–H bonds displayed by most organic molecules, often characterized by similar reactivity and steric accessibility, site-selectivity represents one of the major challenges associated with these processes.

Substituted cycloalkanes are important structural motifs in natural occurring terpenes and derivatives (Figure 1). For the development of synthetically useful procedures for aliphatic C–H bond functionalization, cyclic and polycyclic substrates bearing cyclohexane rings such as menthol, sclareolide, giberellic acid, artemisinin, and their derivatives are customarily employed as model substrates to implement site-selectivity in these processes. Moreover, C–H bond functionalization steps have been successfully employed for the oxidative diversification of polycyclic natural products, providing access to a large array of structures.

Although such complex examples as these have been studied, <sup>2c,4</sup> a general understanding of the factors that govern site-selectivity in undirected C–H bond functionalization of saturated carbocycles is still lacking. Such information would be highly valuable for the preparation of substituted cyclohexanes that are broadly represented in common industrial products (Figure 2).<sup>5</sup>

The reactions of monosubstituted cyclohexanes bearing *tert*-butyl and phenyl have been explored with radical and radical-like hydrogen atom transfer (HAT) reagents such as iodanyl radicals, photoexcited decatungstate (DT\*), cytochrome P450, iron and manganese-oxo species, and methyl-(trifluoromethyl)dioxirane (TFDO), as well as with rhodium and iron carbenes. Figure 3 summarizes previous literature data: C–H bond functionalization occurs selectively at secondary C-3 and C-4 ring positions with P450s, Rh- and

Received: April 19, 2021 Published: June 11, 2021





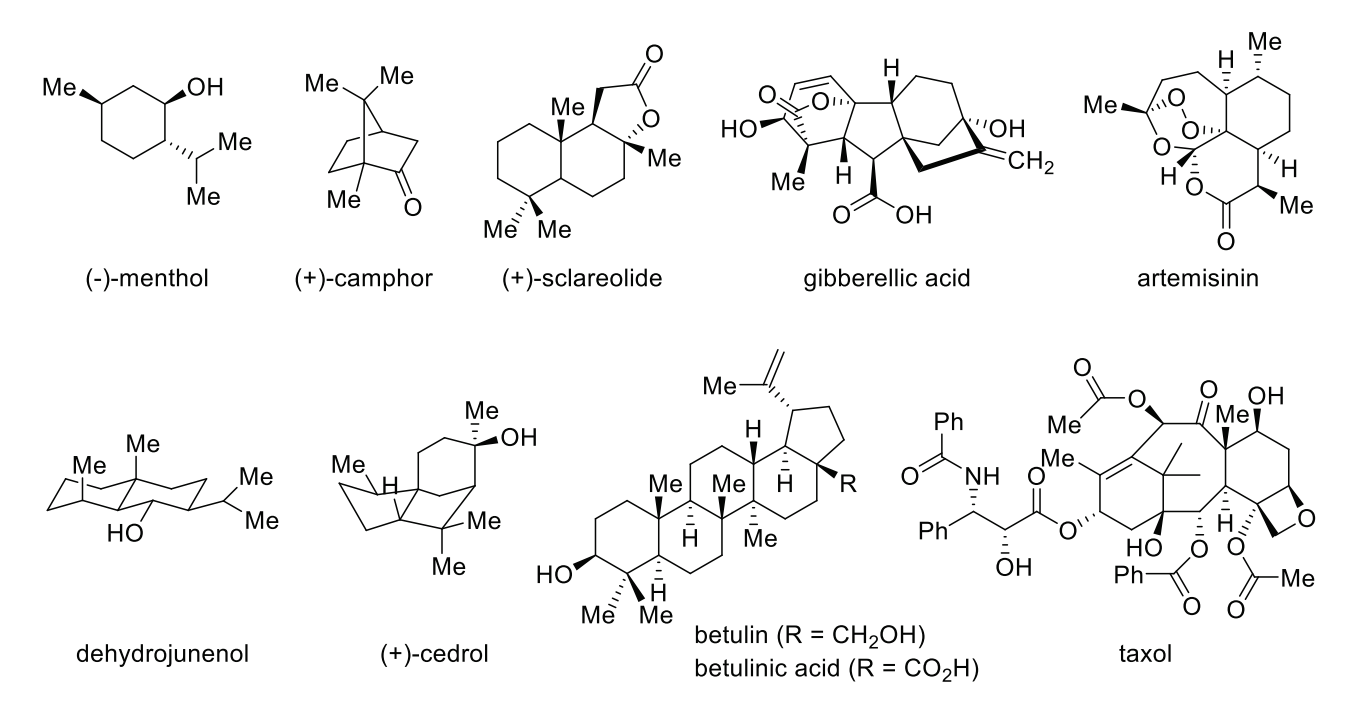


Figure 1. Examples of natural products containing oxygenated cycloalkane rings.

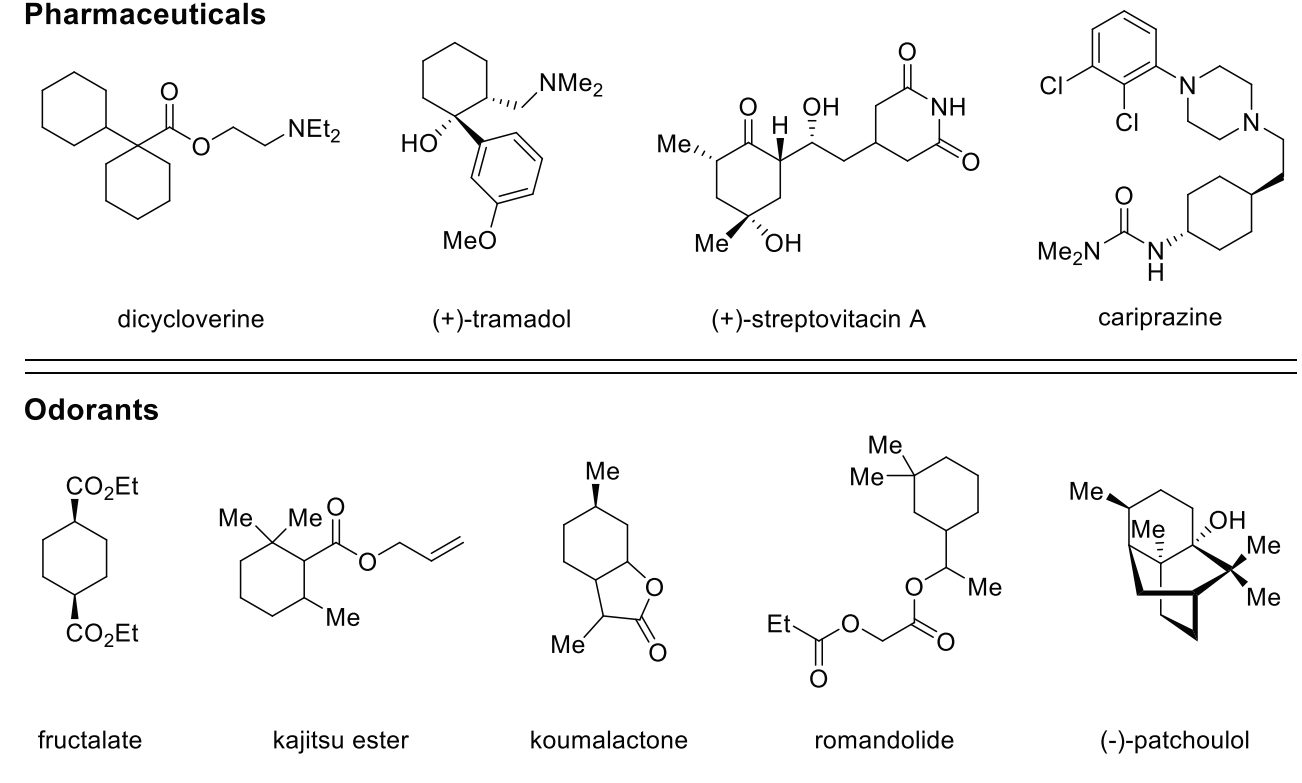
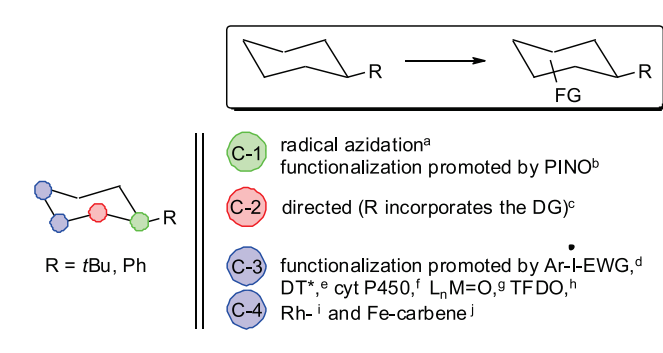


Figure 2. Common industrial products containing substituted cyclohexanes.

Fe-catalyzed carbene insertion, and several radical reagents with limited or no formation of products derived from functionalization at C-1 (i.e., at the intrinsically weaker tertiary C–H bond) or C-2 (Figure 3). On the other hand, azidation<sup>13</sup> of both substrates and functionalization of phenylcyclohexane promoted by the PINO radical<sup>14</sup> have been shown to occur exclusively at C-1. Steric and electronic effects are usually invoked to account for the observed site-selectivity. Selective

functionalization at C-2 of monosubstituted cyclohexanes could only be achieved by means of directed strategies (1,5-HAT, Pd-catalyzed directed by amide functionalities), 15 where the transformation requires however the incorporation of a directing group (DG) into the ring substituent.

Bietti et al. recently proposed an explanation for the selective functionalization at C-3 and C-4 ring positions generally observed in the reaction of *tert*-butylcyclohexane with HAT



**Figure 3.** Summary of the selectivities for radical or radical-like functionalization of monosubstituted cyclohexanes: (a) ref 13; (b) ref 14; (c) ref 15; (d) ref 6; (e) ref 7; (f) ref 8; (g) ref 9; (h) ref 10; (i) ref 11; (j) ref 12.

reagents on the basis of the results obtained with the prototypical HAT reagent CumO<sup>•</sup>.16 A decrease in the second-order rate constant for HAT  $(k_{\rm H})$  was measured on going from cyclohexane and methylcyclohexane to tertbutylcyclohexane. This behavior has been rationalized on the basis of the operation of deactivating torsional effects on HAT from the C-H bonds at C-1 and C-2 ring positions and, in keeping with a decreased reactivity of these bonds, appears to be in line with the site-selectivities observed in the product studies discussed above. In the transition state for HAT from the tertiary axial C-H bond (C-1) to CumO<sup>•</sup>, planarization of the incipient carbon-centered radical forces the C-R bond toward an unfavorable eclipsed interaction with the equatorial C-H bonds at the adjacent positions (Scheme 1A, X =CumO), causing an increase in torsional strain and a corresponding deactivation toward HAT from this site.

Scheme 1. Transition Structures for HAT from the C-H Bonds at C-1 (A) and C-2 (B) of Monosubstituted Cyclohexanes

C-H bond deactivation at C-2 (and C-6) can also be accounted for on the basis of an increase in torsional strain in the HAT transition state, where planarization of the incipient carbon centered radical forces the remaining C-H bond toward an unfavorable eclipsed interaction with the C-R bond at the adjacent position (Scheme 1B). In both cases, the contributions of these deactivating effects are expected to increase with increasing steric bulk of the R group.

In order to provide a deeper understanding of the factors that govern reactivity and site-selectivity in HAT-based C—H bond functionalization of cycloalkane derivatives, and to fully account for the patterns described in Figure 3, we report an experimental and theoretical study of the reactivities and site-selectivities in hydrogen-atom abstraction and C—H oxidative functionalizations of the monosubstituted cyclopentanes and cyclohexanes shown in Scheme 2. Reactions of the cumyloxy radical (CumO•) are compared with those of a reactive dioxirane, ethyl(trifluoromethyl)dioxirane (ETFDO), and in some cases, with the results of previous studies on C—H bond

Scheme 2. Structure of the Substrates and HAT Reagents

azidations and functionalizations promoted by the phthalimide-*N*-oxyl (PINO) radical. Time-resolved kinetics, product studies, and computations of C–H BDEs and reaction barriers described herein have led to a detailed understanding of the selectivities that can be achieved in these reactions.

#### EXPERIMENTAL RESULTS

Reactions with CumO\*. Time-Resolved Kinetic Studies. CumO\* was generated following 355 nm laser flash photolysis (LFP) of argonsaturated acetonitrile or chlorobenzene solutions (T = 25 °C) containing 1.0 M dicumyl peroxide. In these solvents, CumOo is characterized by a broad absorption band in the visible region of the spectrum centered at 485 nm and in the absence of added substrate decays mainly by  $C-CH_3$   $\beta$ -scission. <sup>17</sup> The reactions of CumO $^{\bullet}$  with the different cycloalkanes were studied using the LFP technique following the decay of the CumOo visible absorption band as a function of substrate concentration. The observed rate constants  $(k_{\rm obs})$  gave excellent linear relationships when plotted against substrate concentration, and the second-order rate constants for HAT  $(k_{\rm H})$  were derived from the slope of these plots (see the Supporting Information). The  $k_{\rm H}$  values measured in acetonitrile, for reaction of CumO with cyclopentane, methylcyclopentane, cyclohexane, methylcyclohexane, *tert*-butylcyclohexane, and phenylcyclohexane, are available from previous studies. <sup>16,18,19</sup> Because of the poor solubility of tert-butylcyclopentane in acetonitrile, the reaction of CumO with this substrate has now been studied in chlorobenzene. As a matter of comparison, the reactions of methylcyclopentane and tert-butylcyclohexane were also studied in chlorobenzene, and no kinetic solvent effect was observed. The measured  $k_{\rm H}$  values for reaction of CumO with the substrates displayed in Scheme 2 are collected in Table 1.

Table 1. Second-Order Rate Constants  $(k_{\rm H})$  for Reaction of the Cumyloxyl Radical (CumO $^{\bullet}$ ) with Substituted Cycloalkanes<sup>a</sup>

substrate	$k_{\rm H}~({ m M}^{-1}~{ m s}^{-1})$	ref
cyclopentane	$(9.54 \pm 0.08) \times 10^5$	16
methylcyclopentane	$(1.31 \pm 0.02) \times 10^6$	16
	$(1.32 \pm 0.02) \times 10^{6b}$	this work
tert-butylcyclopentane	$(1.08 \pm 0.03) \times 10^{6b}$	this work
phenylcyclopentane	$(2.05 \pm 0.01) \times 10^6$	this work
cyclohexane	$(1.1 \pm 0.1) \times 10^6$	18
methylcyclohexane	$(1.01 \pm 0.05) \times 10^6$	16
ethylcyclohexane	$(9.8 \pm 0.2) \times 10^5$	this work
isopropylcyclohexane	$(1.17 \pm 0.01) \times 10^6$	this work
tert-butylcyclohexane	$(8.2 \pm 0.3) \times 10^5$	16
	$(8.01 \pm 0.07) \times 10^{5b}$	this work
phenylcyclohexane	$(9.1 \pm 0.2) \times 10^5$	19

<sup>a</sup>Measured in argon-saturated acetonitrile solution at  $T=25\,^{\circ}\mathrm{C}$  employing 355 nm LFP: [dicumyl peroxide] = 1.0 M. <sup>b</sup>Measured in PhCl solution.

Product Studies. Product analysis of the reactions of CumO\* with the cyclopentane and cyclohexane substrates was performed. CumO was generated by 310 nm steady-state photolysis of oxygensaturated acetonitrile or chlorobenzene solutions containing 0.1 M dicumyl peroxide. In the presence of the substrate (0.30 M), HAT from the aliphatic C-H bonds occurs, and the carbon-centered radicals thus formed are rapidly trapped by reaction with oxygen to give peroxyl radical intermediates that evolve to the oxidation products (ketones and secondary and tertiary alcohols, Scheme 3).

## Scheme 3. HAT-Based Aliphatic C-H Bond Oxygenation Promoted by CumO<sup>6</sup>

$$R-H$$
 +  $CumO^{\bullet}$   $\xrightarrow{HAT}$   $R^{\bullet}$  +  $CumO-H$   $R^{\bullet}$  +  $O_2$   $\xrightarrow{}$  alcohols and ketones

The reactions were carried out in acetonitrile at T = 25 °C for an irradiation time of 9 h. Because of the solubility issues discussed above, the reactions of tert-butylcyclopentane have been carried out in chlorobenzene. Full details of these studies and the product distributions thus obtained are reported in the Supporting Information. In the reactions of CumO with methyl-, phenyl-, and tert-butylcycloalkanes, formation of the tertiary alcohol deriving from HAT at C-1 has been observed, accompanied by secondary alcohols and ketones at the other ring positions, derived from HAT at C-2, C-3, and, with cyclohexane substrates, C-4, and from the follow-up oxidation of the first-formed secondary alcohol products (Scheme 4). No evidence for the formation of oxidation products deriving from HAT from the methyl and tert-butyl groups has been obtained, in agreement with the low reactivity displayed by unactivated methyl C-H bonds toward CumO<sup>•.17</sup> Because of the competitive and facile oxidation of the first formed secondary alcohol products, no information on the *cis-trans* stereoselectivity has been obtained.<sup>20,21</sup>

In the reactions of CumO with ethyl- and isopropylcyclohexane, in addition to the above-mentioned products deriving from oxidation at the ring positions, formation of 1-cyclohexylethanol, cyclohexylmethylketone, and 2-cyclohexyl-2-propanol was observed, derived from HAT from side-chain C-H bonds and, with the former substrate, overoxidation of the first formed secondary alcohol product. Because HAT to CumO $^{\bullet}$  occurs in competition with C-CH<sub>3</sub>  $\beta$ -cleavage, cumyl alcohol and acetophenone are always found in the reaction mixture along with these products. In order to simplify product identification and quantitative GC analysis by decreasing the number of products, thus preventing overlap between the GC peaks of structural and stereoisomeric alcohol products, the reaction mixtures have been subjected to follow-up oxidation with chromic acid, which results in the quantitative oxidation of all secondary alcohols into the corresponding ketones, leading to the formation of a single oxidation product (ketone or tertiary alcohol) for each oxidizable position (for details, see the Supporting Information). The product distributions, normalized on a per-hydrogen basis, for reaction of CumO with monosubstituted cyclopentanes and cyclohexanes are displayed in parts A and B, respectively, of Figure 4.

By combining the product distribution for a given monosubstituted cyclopentane or cyclohexane displayed in Figure 4 with the

A Cyclopentanes

**B** Cyclohexanes

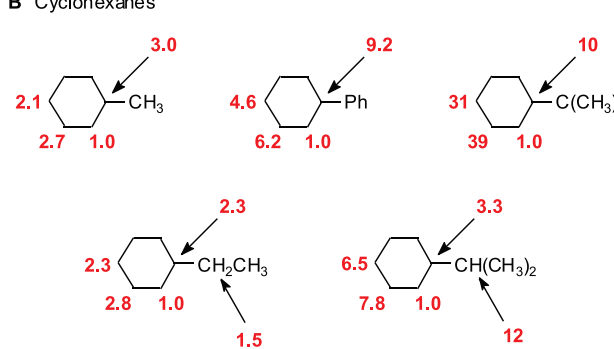


Figure 4. Product ratios on a per-hydrogen basis for reactions of CumO with monosubstituted cyclopentanes and cyclohexanes.

corresponding  $k_{\rm H}$  value (Table 1), it is possible to derive the normalized rate constants  $(k_{\rm H}({\rm norm}))$  for HAT from each site of this substrate to CumO $^{\bullet}$ . The  $k_{\rm H}({\rm norm})$  values obtained for the monosubstituted cyclopentanes and cyclohexanes are collected in Figures 5 and 6, respectively.

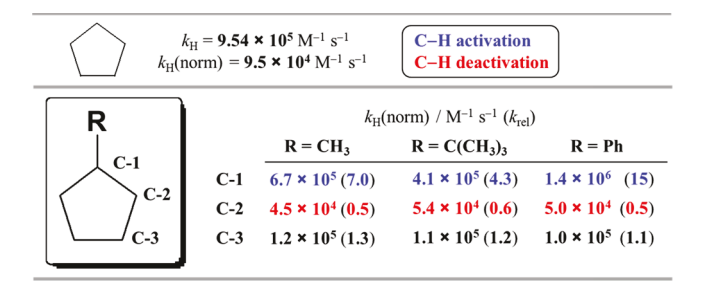


Figure 5. Normalized rate constants  $(k_{\rm H}({\rm norm}))$  for HAT from the C-H bonds of monosubstituted cyclopentanes to the cumyloxyl radical (CumO $^{\bullet}$ ) and reactivity ratios ( $k_{rel}$ ) with respect to cyclopentane.

The degree of activation (in blue) or deactivation (in red) for the C-H bonds of these substrates with respect to cyclopentane and cyclohexane  $(k_{rel})$  can be obtained by comparing these values with the normalized rate constant for HAT from a single secondary C-H bond of these latter substrates ( $k_{\rm H}({\rm norm}) = 9.5 \times 10^4$  and  $9.2 \times 10^4$  M<sup>-1</sup>  $s^{-1}$ , respectively). 10

Computational Results. Conformational searches were carried out by means of Spartan'18 software<sup>22</sup> at the MMFF level, followed by preoptimization of their geometry by the semiempirical PM6<sup>23</sup> method. The structures of reactants and transition states were then optimized using unrestricted calculations with the density functional

#### Scheme 4. Structure of the Products Observed in the Oxygenation of Monosubstituted Cyclopentanes and Cyclohexanes Promoted by CumO<sup>•</sup>

$$R = Me, Ph, tBu$$

$$n = 1,2$$

$$R = Me, Ph, tBu$$

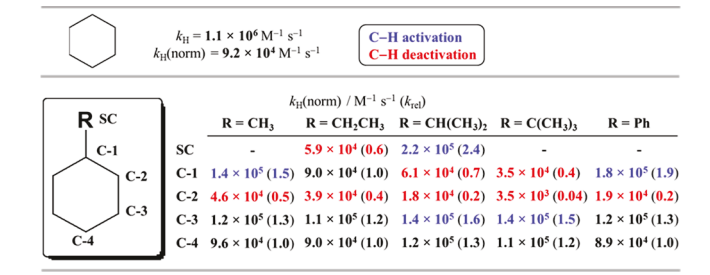


**Figure 6.** Normalized rate constants  $(k_{\rm H}({\rm norm}))$  for HAT from the C–H bonds of monosubstituted cyclohexanes to the cumyloxyl radical (CumO $^{\bullet}$ ) and reactivity ratios  $(k_{\rm rel})$  with respect to cyclohexane.

 $\omega$ B97X-D<sup>24</sup> with the 6-31G (d) basis set. Frequency analyses were carried out on these stationary points to verify that they are energy minima or saddle points (transition states). Single-point energies with a more extensive basis set were carried out with U $\omega$ B97X-D/6-311++G (d, p) on the optimized geometries. The solvent effects for CH<sub>3</sub>CN were included with the CPCM<sup>25</sup> model. All calculations were performed with Gaussian 16.<sup>26</sup>

The DFT activation barriers for reactions of CumO $^{\bullet}$  with a series of monosubstituted cyclopentane and cyclohexane derivatives are listed in Table 2.  $\Delta G^{\ddagger}(cal)$  is the activation barrier for HAT from the C–H bond at a given position. For methylenic sites,  $\Delta G^{\ddagger}(cal)$  represents the activation barriers for the C–H bonds that are *trans* or *cis* to the ring substituent. Also collected in Table 2 are the corresponding C–H BDEs. Full details are provided in Table S6.1.

The transition structures for HAT from the different C-H bonds of monosubstituted cyclopentanes and cyclohexanes to CumO<sup>•</sup> are displayed in Tables 3 and 4, respectively.

In Tables 5 and 6, the calculated activation barriers ( $\Delta G^{\ddagger}(cal)$ ) for the reaction of CumO $^{\bullet}$  with monosubstituted cyclopentanes and cyclohexanes are compared with the corresponding experimental values ( $\Delta G^{\ddagger}(exp)$ ) derived from the  $k_{\rm H}({\rm norm})$  values displayed in Figures 5 and 6, respectively.

The calculations are consistent with the experimental results, with mean absolute errors (MAE) and root mean square errors (RMSE) of 0.76 and 0.96 kcal/mol, respectively. The differences between calculations and experiments are within 1 kcal/mol on average, although larger deviations are found for HAT from C-3 of methylcyclopentane, C-4 of methylcyclohexane, and C-1 and C-2 of tert-butylcyclohexane. Figure 7 shows a correlation between the calculated and experimental values ( $R^2 = 0.79$ ), although there are three outliers (C-2 of phenylcyclohexane, C-2 of tert-butylcyclopentane, and C-1 of methylcyclohexane). The barriers were underestimated by calculations compared with the experimental barriers for these three substrates, while the calculations overestimated the barriers for other substrates (see Tables 5 and 6 and discussion below). The computed barriers are more sensitive to the relative position of the C–H bond than the experimental values.

As a matter of comparison, DFT activation barriers have also been calculated for the reactions of the azide and PINO radicals with both tert-butyl- and phenylcyclohexane, the results for which have been presented above (Figure 3). The  $\Delta G^{\ddagger}(\text{cal})$  values are listed in Table

**Reactions with ETFDO.** Product studies on the reactions of methyl- and *tert*-butycyclopentane and of methyl-, ethyl-, isopropyl-, and *tert*-butylcyclohexane with in situ generated ETFDO were also carried out. For these processes, recent computational studies support a mechanism that proceeds through rate-determining HAT from a substrate C–H bond to the dioxirane, followed by in-cage collapse of the radical pair to give the hydroxylation product and the ketone, precursor of the dioxirane (Scheme 5).<sup>27,28</sup>

ETFDO was generated by a slight modification of a previously described portionwise addition protocol, based on the successive additions of Oxone ( $4 \times 1$  equiv), NaHCO<sub>3</sub> ( $4 \times 4$  equiv), and 1,1,1-trifluoro-2-butanone ( $4 \times 0.2$  equiv) to a 1,1,1,3,3,3-hexafluoro-2-

Table 2. Calculated Activation Barriers ( $\Delta G^{\ddagger}(cal)$ ) for HAT from the C-H Bonds of Cyclopentane and Cyclohexane Derivatives to the Cumyloxyl (CumO $^{\bullet}$ ) Radical and Calculated BDEs for the Corresponding C-H Bonds

Substrate	С-Н	ΔG <sup>‡</sup> (cal) kcal mol <sup>-1</sup>	BDE C-H kcal mol <sup>-1</sup>	
	R = Me C-1	9.9	91.8	
	R = Me C-2 (trans)	12.1	94.3	
	R = Me C-2 (cis)	13.4	94.3	
R	R = Me C-3 (trans)	11.6	93.7	
·1``	R = Me C-3 (cis)	11.7	93.7	
C-1	R = tBu C-1	10.4	91.8	
C-2	R = tBu C-2 (trans)	10.4	94.3	
\/ <sub>C-3</sub>	R = tBu C-2 (cis)	13.9	94.3	
C-3	R = tBu C-3 (trans)	10.9	94.0	
	R = tBu C-3 (cis)	11.0	94.0	
	R = Ph C-1	9.4	80.8	
	R = Ph C-2 (trans)	11.7	93.9	
	R = Ph   C-2  (cis)	13.9	93.9	
	R = Ph C-3 (trans)	11.7	93.9	
	R = Ph C-3 (cis)	14.0	93.9	
	R = Me C-1 (ax)	10.2	94.5	
	R = Me C-2 (trans-eq)	12.0	97.1	
	R = Me C-3 (trans-ax)	11.5	96.7	
R	R = Me C-4 (cis-ax)	11.8	96.7	
C-1	R = tBu C-1 (ax)	12.9	95.0	
C-2	$R = tBu  \mathbf{C-2}  (cis\text{-ax})$	13.8	96.4	
	R = tBu C-3 (cis-eq)	11.4	96.7	
C-3	R = tBu C-4 (cis-ax)	11.8	96.9	
C-4	R = Ph C-1 (ax)	10.5	86.8	
	R = Ph C-2 (trans-eq)	11.4	97.0	
	R = Ph C-3 (trans-ax)	11.4	96.9	
	R = Ph C-4 (cis-ax)	11.5	96.9	
	R = Et C-1 (ax)	10.8	95.1	
	R = Et   C-2  (cis-ax)	11.5	97.0	
	R = Et C-3 (cis-eq)	11.3	96.6	
	R = Et C-4 (cis-ax)	11.7	96.8	

Table 3. Transition Structures along with Calculated Activation Barriers ( $\Delta G^{\ddagger}(cal)$ , Blue Number) for Reactions of the Cumyloxyl Radical (CumO $^{\bullet}$ ) with Monosubstituted Cyclopentanes

Substrate C–H	R = Me	R = Ph	R = tBu
C-1	9.9	9.4	10.4
C-2	12.1	11.7	10.4
C-3	11.6	11.7	10.9

<sup>a</sup>The bond distances for C-H and O-H are in Å; energies are given in kcal/mol.

Table 4. Transition Structures along with Calculated Activation Barriers ( $\Delta G^{\ddagger}(cal)$ , Blue Number) for Reactions of the Cumyloxyl Radical (CumO $^{\bullet}$ ) with Monosubstituted Cyclohexanes<sup>a</sup>

Substrate C-H	R = Me	$\mathbf{R} = \mathbf{E}\mathbf{t}$	R = Ph	$\mathbf{R} = t\mathbf{B}\mathbf{u}$
C-1	10.2	10.8	10.5	12.9
C-2	12.0	11.5	11.4	13.8
C-3	11.5	11.3	11.4	11.4
C-4	11.8	++++** 11.7	11.5	11.8

<sup>&</sup>lt;sup>a</sup>The bond distances for C−H and O−H are in Å; energies are given in kcal/mol.

Table 5. Calculated  $(\Delta G^{\ddagger}(cal))$  and Experimental  $(\Delta G^{\ddagger}(exp))$  Activation Barriers for HAT from the C-H Bonds of Monosubstituted Cyclopentanes to the Cumyloxyl  $(CumO^{\bullet})$  Radical<sup>a</sup>

	ΔG <sup>‡</sup> (cal vs <mark>exp</mark> ) kcal/mol			
R		R=Me	R=tBu	R=Ph
C-1 C-2	C-1	9.9 (9.5)	10.4 (9.8)	9.4 (9.1)
	C-2	12.1 (11.1)	10.4 (11.0)	11.7 (11.1)
	C-3	11.6 (10.5)	10.9 (10.6)	11.7 (10.7)

 $^{\alpha}\Delta G^{\ddagger}(exp)$  is obtained from the Eyring equation based on the normalized rate constants  $(k_{\rm H}({\rm norm}))$  displayed in Figure 5. As a matter of comparison, in the reaction of CumO\* with cyclopentane,  $\Delta G^{\ddagger}(exp)=10.7~{\rm kcal~mol^{-1}},$  obtained from the Eyring equation using the rate constant displayed in Table 1.

propanol (HFIP)/ $H_2O/CH_2Cl_2$  (3.0:1.0:0.75) solvent mixture containing the substrate and  $Bu_4NHSO_4$  (0.05 equiv) at T=0 °C for an overall 48 h reaction time. Full details of these studies are reported in the Supporting Information. Under these conditions, the same oxygenation products observed in the corresponding reactions promoted by the CumO $^{\bullet}/O_2$  system, namely ketones and secondary and tertiary alcohols, are formed. The product distributions, normalized on a per-hydrogen basis, for reaction of ETFDO with monosubstituted cyclopentanes and cyclohexanes are displayed in parts A and B, respectively, of Figure 8.

## DISCUSSION

Starting from the reactions of CumO<sup>•</sup> with the monosubstituted cyclopentanes, the normalized product distributions displayed in Figure 4A show that with all three substrates functionalization predominantly occurs at the tertiary C–H bond. The normalized kinetic data displayed in Figure 5 for

Table 6. Calculated  $(\Delta G^{\ddagger}(cal))$  and Experimental  $(\Delta G^{\ddagger}(exp))$  Activation Barriers for HAT from the C–H Bonds of Monosubstituted Cyclohexanes to the Cumyloxyl (CumO $^{\bullet}$ ) Radical<sup>a</sup>

		ΔG <sup>‡</sup> (cal vs exp) kcal/mol			
		R=Me	R=Et	R=tBu	R=Ph
R LC-1	C-1	10.2 (10.5)	10.8 (10.7)	12.9 (11.0)	10.5 (10.3)
C-2	C-2	12.0 (11.1)	11.5 (11.2)	13.8 (11.7)	11.4 (11.6)
C-4	C-3	11.5 (10.5)	11.3 (10.6)	11.4 (10.5)	11.4 (10.6)
	C-4	11.8 (10.7)	11.7 (10.7)	11.8 (10.6)	11.5 (10.7)

 $^{a}\Delta G^{\ddagger}(exp)$  is obtained from the Eyring equation based on the normalized rate constants  $(k_{\rm H}({\rm norm}))$  displayed in Figure 6. As a matter of comparison, in the reaction of CumO  $^{\bullet}$  with cyclohexane,  $\Delta G^{\ddagger}(exp)=10.7~{\rm kcal~mol}^{-1},$  obtained from the Eyring equation using the rate constant displayed in Table 1.

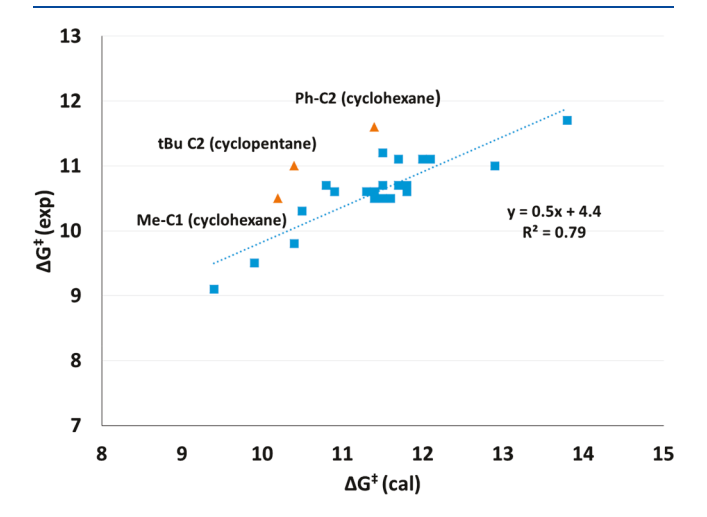


Figure 7. Plot of the activation barriers from DFT calculations  $(\Delta G^{\ddagger}(\text{cal}))$  vs experiment  $(\Delta G^{\ddagger}(\text{exp}))$ . The latter is estimated from the Eyring equation based on the normalized rate constants  $(k_{\text{H}}(\text{norm}))$  obtained by experiment. The orange triangles are the outliers, which have been excluded from the correlation.

CumO<sup>•</sup> show that, as compared to cyclopentane, activation at C-1 is observed for all three substrates, with the degree of activation that significantly increases on going from the tertiary C-H bonds of methyl- and tert-butylcyclopentane ( $k_{rel} = 7.0$ and 4.3, respectively) to the tertiary benzylic C-H bond of phenylcyclopentane ( $k_{\rm rel}$  = 15), in line with the computed BDEs displayed in Table 2. Comparison between the k<sub>H</sub>(norm) values for HAT from cyclopentane and from the C-1-H bond of methyl- and phenylcyclopentane ( $k_{\rm H}({\rm norm})$  =  $9.5 \times 10^4$ ,  $6.7 \times 10^5$ , and  $1.4 \times 10^6$  M<sup>-1</sup> s<sup>-1</sup>, respectively), with those measured for HAT from a secondary C-H bond of pentane,19 and from a tertiary C-H bond of two representative substrates such as 2,3-dimethylbutane and cumene to CumO $^{\bullet}$  ( $k_{\rm H}({\rm norm}) = 5.2 \times 10^4$ ,  $2.8 \times 10^5$  and  $5.6 \times 10^5$  M $^{-1}$  s $^{-1}$ , respectively),  $^{30}$  shows a similar trend for the cyclic and acyclic systems. The cyclopentyl C-H bonds are in all cases more reactive than their acyclic counterparts by a factor ~2. This picture is indicative of a comparable role played by steric effects in the two systems, indicating moreover a negligible role in the cyclopentyl derivatives for deactivating torsional effects such as those depicted in Scheme 1A.

Table 7. Calculated Activation Barriers ( $\Delta G^{\ddagger}(cal)$ ) for HAT from the C-H Bonds of *tert*-Butyl- and Phenylcyclohexane to the Azide ( $N_3^{\bullet}$ ) and Phthalimide-N-oxyl (PINO) Radicals

	( 3 /	, , ,
radical	С-Н	$\Delta G^{\ddagger}(\mathrm{cal})$ (kcal mol <sup>-1</sup> )
$N_3$	R = Ph C-1 (ax)	13.8
	R = Ph C-2 (cis-ax)	18.2
	R = Ph C-2 (trans-eq)	17.4
	R = Ph C-3 (trans-ax)	17.0
	R = Ph C-3 (cis-eq)	17.7
	R = Ph C-4 (cis-ax)	17.5
	R = Ph C-4 (trans-eq)	17.9
	R = tBu C-1 (ax)	14.3
	R = tBu C-2 (cis-ax)	17.8
	R = tBu C-2 (trans-eq)	18.7
	R = tBu C-3 (trans-ax)	17.2
	R = tBu C-3 (cis-eq)	17.2
	R = tBu C-4 (cis-ax)	17.4
	R = tBu C-4 (trans-eq)	17.8
PINO	R = Ph C-1 (ax)	18.6
	R = Ph C-2 (cis-ax)	25.8
	R = Ph C-2 (trans-eq)	25.6
	R = Ph C-3 (trans-ax)	24.5
	R = Ph C-3 (cis-eq)	25.5
	R = Ph C-4 (cis-ax)	23.8
	R = Ph C-4 (trans-eq)	25.1
	R = tBu C-1 (ax)	23.1
	R = tBu C-2 (cis-ax)	25.9
	R = tBu C-2 (trans-eq)	26.4
	R = tBu C-3 (trans-ax)	24.8
	R = tBu C-3 (cis-eq)	24.6
	R = tBu C-4 (cis-ax)	24.0
	R = tBu C-4 (trans-eq)	24.7

Scheme 5. HAT-Based Aliphatic C-H Bond Oxygenation Promoted by Dioxiranes

$$R-H + \bigcup_{R''}^{O} \xrightarrow{R'} \xrightarrow{HAT} R^* + \bigcup_{R''}^{HO} \xrightarrow{R'} R - OH + O = \begin{pmatrix} R' \\ R'' \end{pmatrix}$$

A Cyclopentanes

B Cyclohexanes

**Figure 8.** Product ratios on a per-hydrogen basis for reactions of ETFDO with monosubstituted cyclopentanes and cyclohexanes.

For all three substrates, weak deactivation is observed for the secondary C–H bonds at C-2 ( $k_{\rm rel}=0.5-0.6$ ), while no significant effect is observed for the C–H bonds at C-3. This indicates that HATs from these positions are not influenced by the nature of the ring substituent.

Benzylic activation was observed in both experiments and calculations, which is consistent with the early transition state reflected by the transition structure (the C-H bond distance for R = Ph is 1.22 Å while that for R = Me and tBu is 1.24 Å),

see Table 3. Weak deactivation for C-2 and no significant effect at C-3 were found in experiments, while the calculation overestimates the deactivation effect for C-2 of R = Me and Ph; the deactivation for C-2 of R = tBu was not predicted in calculations (Table 5).

For monosubstituted cyclohexanes, the  $k_{\rm H}$  values measured for HAT to CumO $^{\bullet}$  (Table 1) vary only between  $8.2 \times 10^5$  and  $1.17 \times 10^6$  M $^{-1}$  s $^{-1}$ . Normalized product distributions and rate constants displayed in Figure 4B and Figure 6 show that the nature of the ring substituent strongly impacts on the reactivity of the C $^{-}$ H bonds at C $^{-1}$  and C $^{-2}$ . The rate constant for HAT from the tertiary C $^{-}$ H bond (C $^{-1}$ ) decreases on going from methyl- and phenylcyclohexane to ethyl-, isopropyl-, and *tert*-butylcyclohexane, and the relative importance of HAT from C $^{-2}$  decreases sharply with increasing steric bulk of the ring substituent. Competitive HAT from sidechain (SC) C $^{-}$ H bonds is observed only with ethyl- and isopropylcyclohexane, with the relative importance of this pathway increasing on going from the former to the latter substrate, that is, with decreasing C $^{-}$ H BDE in the substituent.

For cyclohexane,  $k_{\rm H}({\rm norm}) = 9.2 \times 10^4 {\rm M}^{-1} {\rm s}^{-1},^{16}$  and a slight increase in the rate constant for HAT from C-1 is only observed for methyl- and phenylcyclohexane ( $k_{\rm rel}$  = 1.5 and 1.9, respectively). An up to 2.5-fold decrease in  $k_{\rm H}({\rm norm})$  is observed for isopropyl- and tert-butylcyclohexane ( $k_{rel} = 0.7$ and 0.4, respectively). These values are in all cases lower than the values obtained for HAT from the tertiary C-H bonds of representative acyclic substrates such as 2,3-dimethylbutane and cumene  $(k_{\rm H}({\rm norm}) = 2.8 \times 10^5 \text{ and } 5.6 \times 10^5 \text{ M}^{-1} \text{ s}^{-1})$ respectively), 30 with a value for HAT from the exocyclic tertiary C-H bond of isopropylcyclohexane ( $k_{\rm H}({\rm norm}) = 2.2$  $\times$  10<sup>5</sup> M<sup>-1</sup> s<sup>-1</sup>) that is only slightly lower than that from 2,3dimethylbutane. The tertiary C-H bonds of the corresponding cyclopentane derivatives discussed above have  $k_{rel}$  (cyclopentane/cyclohexane) = 4.8, 11.7, and 7.8, respectively, for R = Me, tBu, and Ph, pointing toward a certain extent of deactivation for the tertiary C-H bonds of the cyclohexanes.

Deactivation is also observed for the secondary C–H bonds at C-2, with the  $k_{\rm H}({\rm norm})$  value that decreases with increasing steric bulk of the ring substituent approaching a factor 20 ( $k_{\rm rel}$  = 0.04) with *tert*-butylcyclohexane.

Comparison of the results obtained in the reactions of CumO\* with the monosubstituted cyclopentanes and cyclohexanes indicates that C-H bond deactivation at C-1 and C-2 cannot be accounted for on the basis of steric effects but instead is a result of the deactivating torsional effects discussed above (Scheme 1) that operate mainly in the cyclohexane derivatives.

With all monosubstituted cyclohexanes, no significant effect is observed for the C-3 and C-4 C-H bonds; a slightly higher reactivity is observed for C-3 C-H bonds as compared to the latter ones. The C-3/C-4 reactivity ratio is not influenced to any significant extent by the nature of the ring substituent.

Calculations overestimate the activation barriers for HAT from C-3 and C-4 for all the R-groups, but consistent trends are found from both calculations and experiments: (1) deactivation at C-1 and C-2 for R = tBu; (2) no benzylic activation for R = Ph; (3) constant barriers at C-3 and C-4 and constant C-3/C-4 reactivity ratio irrespective of the nature of R

The transition structures for the reactions of CumO $^{\bullet}$  with the monosubstituted cyclohexanes are displayed in Table 4. The C-H bond lengths at C-1 for R = Me, Et, and tBu are

1.25, 1.26, and 1.27 Å, respectively, indicating a slightly later position of the transition state along the reaction coordinate. Although an earlier transition state was indicated for HAT from C-1 of phenylcyclohexane by the transition structure displayed in Table 4, no evidence for benzylic activation was obtained. Our calculations show that the BDE for the C-1—H bond of phenylcyclopentane and phenylcyclohexane are 80.8 and 86.8 kcal/mol, respectively, and the lower BDE is consistent with the lower activation barrier for the cyclopentane system. As compared to phenylcyclopentane, the lack of benzylic activation at C-1 for phenylcyclohexane may thus arise from both the deactivating torsional effects discussed above and the less favorable C—H BDE.

Table 4 shows that in the transition state the phenyl group of phenylcyclohexane has a different orientation for HAT from the C-1—H bond than from the other sites. The activation energy at C-3 of Me and Ph is lower for HAT from the axial position, while abstraction at C-3 of Et and *t*Bu is preferred from the equatorial C—H bond. The C-4 transition structures are very similar regardless of the nature of R, resulting in very similar activation barriers.

This mechanistic picture is nicely supported by the results obtained in the oxidation of the alkyl-substituted cyclopentanes and cyclohexanes by ETFDO displayed in Figure 8. Previous studies have shown that aliphatic C–H bond oxidation promoted by dioxiranes selectively occurs at tertiary over secondary sites, <sup>29,31</sup> and computational studies support a mechanism that proceeds through rate-determining HAT. <sup>27,28</sup> Along this line, in the reactions of ETFDO with methyl- and *tert*-butylcyclopentane, oxidation predominantly occurs at the tertiary C–H bond, with normalized site-selectivity trends at C-1, C-2 and C-3 of 70:1:1.9 and 42:1:1.7, respectively that parallel those observed in the corresponding reactions with CumO<sup>•</sup> displayed in Figure 4A (15:1:2.6 and 7.5:1:2.1), although with significantly higher selectivity for the tertiary site.

With the cyclohexane derivatives (Figure 8B), high selectivity for tertiary C-H bond oxidation is only observed for methylcyclohexane, with selectivity for this site that decreases on going from methyl- to ethyl-, isopropyl-, and tert-butylcyclohexane, that is, with increasing steric bulk of the ring substituent. This is in line with the results obtained in the corresponding reactions with CumO (Figure 4B). The product distributions obtained with methyl- and tertbutylcyclohexane are in good agreement with those obtained previously in the oxidation of the same substrates with TFDO.<sup>10</sup> As a matter of comparison, the normalized C-1/C-2 product ratio decreases by a factor ~1.7 on going from methylto tert-butylcyclopentane and by a factor ~24 for the corresponding cyclohexane couple. These results are indicative of the strong deactivation toward HAT for the tertiary C-H bond of tert-butylcyclohexane and support once again the important role played by torsional effects in these reactions.

In the reaction of isopropylcyclohexane, oxidation of the exocyclic tertiary C–H bond outcompetes oxidation of the endocyclic one by a factor 8. Among the cyclohexane series, deactivation at C-2 is only observed with *tert*-butylcyclohexane, a behavior that contrasts with that observed with CumO• and that reasonably reflects the greater steric demand of this HAT reagent as compared to ETFDO.

With these results in hand, it is possible to rationalize the site-selectivities observed in previous studies on HAT-based functionalization of phenyl- and *tert*-butylcyclohexane pro-

moted by radical and radical-like reagents summarized in Figure 3, in terms of the relative contribution of C-H bond strengths and torsional effects.

The BDEs of  $H-N_3$  and PINO-H are 93.3 and 88.1 kcal mol<sup>-1</sup>, respectively. The calculated C-H BDEs are 95.0 and 86.8 kcal mol<sup>-1</sup> for the tertiary C-H bond of tertbutylcyclohexane and phenylcyclohexane, respectively. The BDEs for the secondary C-H bonds of both substrates are 96–97 kcal mol<sup>-1</sup> (Table 2). The activation barriers (Table 7) show that HAT from the secondary C-H bonds of both substrates to N<sub>3</sub> and PINO and from the tertiary C-H bond of tert-butylcyclohexane to PINO are thermodynamically and kinetically unfavorable, supporting the experimental observation that functionalization selectively occurs at the weaker tertiary C–H bond. 13,14 On the other hand, with reagents such as CumO<sup>•</sup>, DT\*, <sup>7</sup> cytochrome P450, <sup>8</sup> iron and manganese-oxo species,9 and dioxiranes,10 HAT is accompanied by the formation of a relatively strong O-H bond (BDE ~ 100-105 kcal mol<sup>-1</sup>). In these cases, abstraction from all ring positions becomes thermodynamically favorable, and torsional effects dictate the observed site-selectivity. This accounts, together with steric effects for the more bulky reagents, for the observed C-H bond deactivation at C-1 and C-2.

## CONCLUSIONS

Time-resolved kinetic, product and computational studies on the reactions of CumO with alkyl- and phenyl-substituted cyclopentanes and cyclohexanes, combined with product studies on the reactions of some of these substrates with ethyl(trifluoromethyl)dioxirane, have led to quantitative information on the reactivity and selectivity patterns observed in C-H bond oxygenation of saturated carbocycles. The important role played by torsional strain in these reactions is highlighted. We provide useful guidelines to be implemented in the development of procedures for aliphatic C-H bond functionalization of cycloalkane motifs. Significantly different behavior is observed for the cyclopentane and cyclohexane derivatives. With the former substrates, the expected trends have been observed: functionalization predominantly occurs at the most activated tertiary C-H bond, with steric and torsional effects that appear to play a minor role in governing reactivity and site-selectivity. With the cyclohexane substrates, which exist in more rigid chair geometries, the nature of the ring substituent strongly impacts the reactivity of the C-H bonds at C-1 and C-2. The extent of deactivation toward HAT increases with increasing steric bulk of the ring substituent, shifting progressively functionalization to C-3 and C-4 ring positions. The observed deactivation can be accounted for on the basis of an increase in torsional strain in the transition states for HAT from C-1 and C-2 of these substrates. These results are well supported by the site-selectivities observed in the oxidation of the same substrates promoted by ethyl-(trifluoromethyl)dioxirane, pointing toward torsional effects as a major determinant in governing site-selectivity in the reaction of oxygen-centered HAT reagents with monosubstituted cyclohexanes. By combining the results obtained in this study with those obtained previously for HAT-based C-H bond azidation and functionalizations promoted by the PINO radical, a general framework for the mechanistic description of HAT based C-H bond functionalizations of cycloalkanes has been obtained. We show that phenyl- and tert-butylcycloalkanes are useful mechanistic probes for an understanding of the factors that govern selectivity in these reactions.

#### **■ EXPERIMENTAL SECTION**

**General Methods.** Gas-chromatographic analyses were carried out with a Varian CP 3800 gas chromatograph equipped with a 30 m  $\times$  0.25 mm CP-Sil 5 CB or a 30 m  $\times$  0.25 mm ZB-5Ms plus capillary column. GC–MS analyses were carried out with a HP5890 series II plus gas-chromatograph equipped with a 30 m  $\times$  0.25 mm CP-Sil 5 CB capillary column and coupled with a HP 5972 MSD mass spectrometer. <sup>1</sup>H NMR and <sup>13</sup>C NMR spectra were recorded on Bruker Avance 400 MHz and Bruker Avance 700 MHz spectrometers. Spectra are referenced to tetramethylsilane (TMS).

Laser Flash Photolysis Studies. Time-resolved kinetic studies were carried out by laser flash photolysis (LFP) employing a laser kinetic spectrometer using the third (355 nm) harmonic of a Qswitched Nd:YAG laser delivering pulses of the duration of 8 ns. The laser energy was adjusted to ≤10 mJ/pulse by use of an appropriate filter. A 3.5 mL Suprasil quartz cell (10 mm × 10 mm) was used, and all of the experiments were carried out at  $T = 25 \pm 0.5$  °C under magnetic stirring. Experiments have been typically carried out employing argon- or nitrogen-saturated acetonitrile or PhCl solutions containing 1.0 M dicumyl peroxide. The observed rate constants  $(k_{\text{obs}})$  were obtained following the decay of the cumyloxyl radical (CumO\*) absorption band at 490 nm as a function of the concentration of added substrate. Second-order rate constants  $(k_{\rm H})$ for the reactions of CumO with the substrates were obtained from the slopes of the  $k_{\rm obs}$  vs [substrate] plots. The  $k_{\rm H}$  values are the average at least two values obtained through independent experiments, with typical errors being ≤10%. The intercepts of the plots  $(k_0)$  reflect the kinetic contribution of the reactions of CumO $^{\bullet}$  in the absence of substrate.

Oxidation Reactions Promoted by the Cumyloxyl Radical (CumO°). Steady-state photolysis experiments were carried out employing a Helios Italquartz photoreactor, equipped with 10 × 15 W lamps with emission at  $\lambda_{\rm max} = 310$  nm. The reactions were carried out at constant temperature (T = 25 °C) by means of a Haake DC 10 thermostat linked to the outer casing of a Pyrex glass vessel containing the reaction mixture. A 5 mL solution of the substrate (0.3 M) and dicumyl peroxide (135.2 mg, 0.1 M) in acetonitrile or chlorobenzene was introduced in a jacketed glass or quartz tube. The solution was carefully saturated with oxygen and irradiated with 10 × 15 W UV lamps (emission maximum at 310 nm) for 9 h under stirring at T = 25°C. The internal standard (4-tert-butylcyclohexanone (phenylcyclohexane in the reaction of tert-butylcyclohexane)) was then added and the solution directly analyzed without any workup. GC analysis of the solution afforded the conversions of the substrate and product yields relative to the internal standard integration. Oxidation products were identified by comparison with authentic samples of commercially available or synthesized compounds previously characterized and confirmed by GC-MS. For each substrate, the given results are the average of at least three independent experiments.

Oxidation Reactions Promoted by Ethyl(trifluoromethyl)dioxirane (ETFDO). Dioxirane-promoted oxidations were carried out under magnetic stirring at constant temperature (T = 0 °C) by means of a Julabo F34 refrigerated circulator connected to the outer casing of a Pyrex glass vessel containing the reaction mixture. A 62 mg (0.1 mmol, 1 equiv) portion of potassium peroxymonosulfate triple salt (2KHSO<sub>5</sub> KHSO<sub>4</sub> K<sub>2</sub>SO<sub>4</sub>, oxone) and 33 mg (0.4 mmol, 4 equiv) of NaHCO3 were placed in a Pyrex glass tube equipped with an outer container for circular refrigeration, and then 1.0 mL of bidistilled water was added. When the salts solubilized, 1.7 mg (0.005 mmol, 5 mol %) of Bu<sub>4</sub>NHSO<sub>4</sub>, 3 mL of 1,1,1,3,3,3-hexafluoro-2-propanol (HFIP), and 0.75 mL of dichloromethane were added, followed by 0.1 mmol (1 equiv) of substrate. After 5 min, 3  $\mu$ L (0.02 mmol, 20 mol %) of 1,1,1-trifluoro-2-butanone was added to the reaction mixture. Additional portions of Oxone (1 equiv), NaHCO<sub>3</sub> (4 equiv), and the ketone (20 mol %) were added to the reaction vessel after 5, 10, and 24 h. The reaction was left at T = 0 °C under magnetic stirring for a total time of 48 h. The mixture was then diluted with a saturated NaCl solution and, after addition of an internal standard (4tert-butylcyclohexanone (phenylcyclohexane in the reaction of tertbutylcyclohexane)), extracted with 3 × 5 mL of CH<sub>2</sub>Cl<sub>2</sub>, dried over

anhydrous Na<sub>2</sub>SO<sub>4</sub>, and filtered. GC analysis of the solution afforded the conversion of the substrate and product yields relative to the internal standard integration. Oxidation products have been identified by comparison with authentic samples of commercially available or synthesized compounds previously characterized and confirmed by GC–MS.

Chromic Acid Oxidation of the Reaction Mixtures. Both the CumO\*- and ETFDO-mediated oxidation of substituted cycloalkanes gave mixtures of alcohol and ketone products. These products display very similar spectroscopic and chromatographic properties, and special care should therefore be taken in order to perform the qualitative and quantitative analysis of the reaction mixture. In order to simplify product identification and quantitation procedures decreasing the number of products, the reaction mixtures have been subjected to further oxidization with chromic acid, resulting in the oxidation of all the secondary alcohols into the corresponding ketones. Chromic acid oxidation of the reaction mixtures has been carried out following a procedure reported in the literature. 34

**Materials.** Solvents used were of commercially available reagent quality unless stated otherwise. Spectroscopic grade acetonitrile (MeCN) and chlorobenzene (PhCl) were employed for LFP experiments. Chlorobenzene and dichloromethane were purified and dried before use by filtration over an activated alumina column.

Reagents. Commercially available dicumyl peroxide (≥98%) was used without further purification in all of the time-resolved kinetic and steady-state photolysis studies. All reagents used for synthetic purposes and product studies are commercially available and used as received.

**Substrates.** Methylcyclopentane, methylcyclohexane, ethylcyclohexane, isopropylcyclohexane, *tert*-butylcyclohexane, and phenylcyclohexane were used as received.

tert-Butylcyclopentane was synthesized according to the following sequence by adapting a strategy proposed by Miller, <sup>35</sup> leading to an overall 35% product yield over the four steps. The previously reported synthetic procedures were either very low yielding and run under harsh reaction conditions <sup>36</sup> or afforded the desired product within a complex mixture of isomeric alkanes. <sup>37</sup>

- (a) Synthesis of Dimethyl 2-Cyclopentyl-2-methylmalonate. To a 3neck flame-dried flask containing a magnetic stirring bar, equipped with a condenser and a dropping funnel, was added 1.45 g of NaH (80% in mineral oil, 40.0 mmol, 1.6 equiv) and the mixture washed three times with hexane to remove the mineral oil. THF (50 mL) was then added under Ar. At T = 0 °C, 4.6 mL of dimethyl 2cyclopentylmalonate (24.9 mmol) dissolved in 30 mL of THF was added dropwise to the NaH solution, followed by 2.7 mL of MeI (40.0 mmol, 1.6 equiv). The solution was then heated in an oil bath to 55 °C and stirred for 18 h. After this time, GC analysis showed the complete conversion of the substrate. The reaction mixture was cooled to rt, quenched with 1.0 M HCl, and extracted three times with 30 mL of DCM. The organic layers were collected, dried over anhydrous Na<sub>2</sub>SO<sub>4</sub>, filtered, and dried in vacuo to give 4.7 g (22 mmol, 88% yield) of dimethyl 2-cyclopentyl-2-methylmalonate as a brownish oil. The crude material was used in the following step without further purification. <sup>1</sup>H NMR (CDCl<sub>3</sub>, 400 MHz) δ: 3.71 (m, 6H), 2.54 (m, 1H), 1.71 (m, 2H), 1.56 (m, 6H), 1.38 (s, 3H).
- (b) Synthesis of 2-Cyclopentyl-2-methylpropane-1,3-diol. To a 3-neck flame-dried flask containing 1.9 g of LiAlH<sub>4</sub> (50 mmol, 2.3 equiv) equipped with a dropping funnel containing a magnetic stirring bar under Ar 30 mL of anhydrous THF (30 mL) were added, and the system was cooled to 0 °C. Dimethyl 2-cyclopentyl-2-methylmalonate (4.7 g, 22 mmol) dissolved in 50 mL of THF was successively added dropwise to the LiAlH<sub>4</sub> solution. At the end, the mixture was warmed to rt and analyzed by GC. After complete conversion of the substrate (19 h), the reaction was quenched with 1.0 M HCl and extracted three times with 25 mL of DCM. The organic layers were collected, dried with anhydrous Na<sub>2</sub>SO<sub>4</sub>, filtered, and dried in vacuo to give 2.95 g (18.6 mmol, 85% yield) of 2-cyclopentyl-2-methylpropane-1,3-diol as a white solid (GC purity >99%). <sup>1</sup>H NMR (CDCl<sub>3</sub>, 400 MHz)  $\delta$ : 3.60 (m, 4H), 2.46 (bs, 2H), 2.04 (m, 1H), 1.57 (m, 6H), 1.26 (m, 2H), 0.76 (s, 3H).

(c) Synthesis of 2-Cyclopentyl-2-methylpropane-1,3-diyl Bis-(trifluoromethanesulfonate). A general procedure for triflation of alcohols, reported in the literature, 38 was followed. To a 3-neck flame-dried flask containing a magnetic stirring bar and equipped with a dropping funnel were added 6.64 mL of triflic anhydride (Tf<sub>2</sub>O: 39.5 mmol, 2.5 equiv) followed by 25 mL of DCM under Ar at T = 0°C. A solution of 3.17 mL of pyridine (39.5 mmol, 2.5 equiv) and 2cyclopentyl-2-methylpropane-1,3-diol (2.5 g, 15.8 mmol) dissolved in 25 mL of DCM was then added dropwise to the Tf<sub>2</sub>O solution. The mixture was successively warmed to rt and followed by GC analysis. After complete conversion of the substrate (2 h), the reaction was quenched with water and extracted three times with 30 mL of DCM. The organic layers were collected, dried with anhydrous Na<sub>2</sub>SO<sub>4</sub>, filtered, and dried in vacuo to give 6.60 g (15.6 mmol, 99% yield) of a brown solid containing the crude product. 2-Cyclopentyl-2-methylpropane-1,3-diylbis(trifluoromethanesulfonate) has been identified by <sup>1</sup>H NMR analysis and used in the following step without further purification. <sup>1</sup>H NMR (CDCl<sub>3</sub>, 400 MHz) δ: 4.38 (s, 4H), 1.98 (m, 1H), 1.64 (m, 6H), 1.32 (m, 2H), 0.99 (s, 3H).

(d) Synthesis of tert-Butylcyclopentane. To a 3-neck flame-dried flask equipped with a dropping funnel and containing 5.0 g of 2cyclopentyl-2-methylpropane-1,3-diylbis(trifluoromethanesulfonate) (12 mmol) in 50 mL of THF under stirring was added 40 mL of a 1.0 M solution of LiBHEt<sub>3</sub> in THF (40 mmol) dropwise under Ar at T =0 °C. The mixture was then warmed to rt and followed by GC analysis. After 1 h, quantitative conversion of the substrate was observed and the reaction was quenched with 1.0 M HCl and extracted three times with 35 mL of pentane. The organic layers were collected, dried with anhydrous Na2SO4, and filtered. Because of the relatively low boiling point of the product, special care was taken during the purification procedures. Pentane and THF were distilled away from the mixture at ordinary pressure, and the crude material was then purified by silica gel column chromatography using pentane as eluent. Pentane was distilled away once again at ordinary pressure and the product dried in vacuo at 0 °C, yielding 770 mg (6.1 mmol, 41% yield) of pure tert-butylcyclopentane. Spectroscopic and spectrometric data are consistent with those previously reported in the literature.  $^{37}$  <sup>1</sup>H NMR (CDCl<sub>3</sub>, 700 MHz)  $\delta$ : 1.61 (m, 1H), 1.56 (m, 4H), 1.49 (m, 2H), 1.22 (m, 2H), 0.84 (s, 9H). <sup>13</sup>C NMR{<sup>1</sup>H} (CDCl<sub>3</sub>, 100 MHz)  $\delta$ : 51.1, 32.1, 27.8, 27.4, 26.0. GC–MS m/z: 126 (M<sup>+</sup>), 111, 69, 68, 57, 56 (100).

Phenylcyclopentane was obtained by Friedel–Crafts alkylation of benzene following a procedure reported in the literature. <sup>39</sup>  $^{1}$ H NMR (CDCl<sub>3</sub>, 400 MHz)  $\delta$ : 7.28–7.14 (m, 5H), 3.04–2.93 (m, 1H), 2.07–2.01 (m, 2H), 1.80–1.50 (m, 6H).

**Reaction Products.** The following reaction products are commercial samples of the highest quality available and were used as received: 1-methylcyclopentanol, *trans*-2-methylcyclopentanol, 2-methylcyclopentanone, 3-phenylcyclopentanone, 1-methylcyclohexanol, 2-methylcyclohexanone, *trans*-2-methylcyclohexanol, 3-methylcyclohexanone, *cis*-4-methylcyclohexanol, *trans*-4-methylcyclohexanol, 4-methylcyclohexanone, cyclohexyl methyl ketone, 4-ethylcyclohexanol (*cis*-*trans* mixture), 4-ethylcyclohexanone, 4-isopropylcyclohexanol (*cis*-trans mixture), 4-isopropylcyclohexanone, 4-tert-butylcyclohexanol, *trans*-4-tert-butylcyclohexanol, *trans*-2-phenylcyclohexanol, 4-phenylcyclohexanone.

Authentic samples of 1-tert-butylcyclopentanol, 1-phenylcyclopentanol, 1-ethylcyclohexanol, 1-isopropylcyclohexanol, 1-tert-butylcyclohexanol, and 1-phenylcyclohexanol were available in our laboratory from previous studies.<sup>40</sup>

2-Cyclohexyl-2-propanol was prepared by reaction of cyclohexyl methyl ketone with ethylmagnesium chloride in anhydrous tetrahydrofuran according to a procedure reported in the literature. 41

In order to compare reaction products with authentic samples by GC analysis, *cis-trans* mixtures of secondary alcohols were obtained by reduction with NaBH<sub>4</sub> of available ketones

Characterization of the Oxidation Products. 1-Methylcyclopentanol. GC-MS m/z (relative abundance): 100 ( $M^+$ ), 85, 83, 71 (100), 58, 57, 55. Data are consistent with those obtained from the analysis of a commercially available sample.

2-Methylcyclopentanone. GC-MS m/z (relative abundance): 98 (M<sup>+</sup>), 83, 69, 56, 55, 42 (100), 39. Data are consistent with those obtained from the analysis of a commercially available sample.

3-Methylcyclopentanone. GC-MS m/z (relative abundance): 98 (M<sup>+</sup>), 83, 70, 69, 56, 55, 42 (100), 41, 39. Data are consistent with those reported in the literature.<sup>42</sup>

trans-1-Methylcyclopentane-1,2-diol. GC–MS m/z (relative abundance): 116 (M<sup>+</sup>), 98, 83, 73, 69, 57 (100). Data are consistent with those reported in the literature.<sup>43</sup>

2-Hydroxy-2-methylcyclopentanone. GC-MS m/z (relative abundance): 114 (M<sup>+</sup>), 98, 83, 73, 69, 57 (100), 41. Data are consistent with those reported in the literature.<sup>44</sup>

1-tert-Butylcyclopentanol. GC-MS m/z (relative abundance): 109, 85 (100), 67, 57. Data are consistent with those obtained from the analysis of an authentic sample that was present in our laboratory from previous studies.<sup>40</sup>

2-tert-Butylcyclopentanone. GC–MS m/z (relative abundance): 140 (M<sup>+</sup>), 125, 97, 84, 78 (100), 57, 55, 41. Data are consistent with those reported in the literature.<sup>45</sup>

*3-tert-Butylcyclopentanone.* GC–MS m/z (relative abundance): 140 (M<sup>+</sup>), 125, 97, 84, 69, 57 (100), 55, 41. Data are consistent with those reported in the literature.<sup>46</sup>

1-Phenylcyclopentanol. GC-MS m/z (relative abundance): 162 (M<sup>+</sup>), 144, 133 (100), 128, 115, 105, 98, 78, 77, 55. Data are consistent with those obtained from the analysis of an authentic sample that was present in our laboratory from previous studies.<sup>40</sup>

2-Phenylcyclopentanone. GC-MS m/z (relative abundance): 160 (M $^+$ ), 145, 117, 105, 104 (100). Data are consistent with those reported in the literature.  $^{47}$ 

3-Phenylcyclopentanone. GC-MS m/z (relative abundance): 160 (M+), 142, 131, 128, 120, 117, 115, 105 (100), 100. Data are consistent with those obtained from the analysis of a commercially available sample.

*trans-1-Phenylcyclopentane-1,2-diol.* GC–MS m/z (relative abundance): 178 (M<sup>+</sup>), 133, 105, 77. Data are consistent with those reported in the literature.<sup>48</sup>

 $2\text{-Hydroxy-}2\text{-}phenylcyclopentanone.}$  GC-MS m/z (relative abundance): 176 (M<sup>+</sup>), 148, 133, 129, 120, 115, 105. Data are consistent with those reported in the literature.  $^{49}$ 

1-Methylcyclohexanol. GC-MS m/z (relative abundance): 114 (M<sup>+</sup>), 99, 85, 81, 72, 71 (100), 59, 58, 57, 55, 43. Data are consistent with those obtained from the analysis of a commercially available sample.

2-Methylcyclohexanone. GC-MS m/z (relative abundance): 112 (M+), 97, 95, 85, 84, 81, 69 (100). Data are consistent with those obtained from the analysis of a commercially available sample.

3-Methylcyclohexanone. GC-MS m/z (relative abundance): 112 (M<sup>+</sup>), 97, 95, 84, 83, 79, 69 (100). Data are consistent with those obtained from the analysis of a commercially available sample.

4-Methylcyclohexanone. GC-MS m/z (relative abundance): 112 (M<sup>+</sup>), 97, 95, 84, 83, 79, 69, 58, 55 (100). Data are consistent with those obtained from the analysis of a commercially available sample.

Cyclohexyl methyl ketone. GC-MS m/z (relative abundance): 126 (M<sup>+</sup>), 111, 84, 71, 68, 67, 55 (100). Data are consistent with those obtained from the analysis of a commercially available sample.

1-Ethylcyclohexanol. GC-MS m/z (relative abundance): 128 (M<sup>+</sup>), 99 (100), 85, 81, 72, 69, 55. Data are consistent with those obtained from the analysis of an authentic sample that was present in our laboratory from previous studies.<sup>40</sup>

2-Ethylcyclohexanone. GC-MS m/z: 126 (M<sup>+</sup>), 111, 97, 83, 69, 67, 55 (100). Data are consistent with those reported in the literature. <sup>50</sup>

3-Ethylcyclohexanone. GC-MS m/z: 126 (M<sup>+</sup>), 111, 98, 97, 83 (100), 70, 55. Data are consistent with those reported in the literature.<sup>51</sup>

4-Ethylcyclohexanone. GC–MS m/z: 126 (M<sup>+</sup>), 111, 108, 98, 83, 70, 67, 56, 55 (100). Data are consistent with those obtained from the analysis of a commercially available sample.

2-Cyclohexyl-2-propanol. GC-MS m/z (relative abundance): 142 (M+), 130, 124, 120, 115, 109 (100), 100. Data are consistent with

those obtained from the analysis of an authentic sample that was synthesized as descrived above.

1-Isopropylcyclohexanol. GC–MS m/z (relative abundance): 128, 110, 99 (100), 95, 91, 85, 81, 71, 55, 41. Data are consistent with those obtained from the analysis of an authentic sample that was present in our laboratory from previous studies.<sup>40</sup>

*2-Isopropylcyclohexanone.* GC–MS m/z (relative abundance): 140 (M<sup>+</sup>), 126, 98 (100), 83, 69, 55. Data are consistent with those reported in the literature.<sup>52</sup>

3-Isopropylcyclohexanone. GC-MS m/z (relative abundance): 140 (M<sup>+</sup>), 122, 107, 98, 97 (100), 82, 69, 55, 41. Data are consistent with those reported in the literature. <sup>53</sup>

*4-Isopropylcyclohexanone.* GC–MS m/z (relative abundance): 140 (M<sup>+</sup>), 125, 122, 112, 107, 97, 93, 84, 79, 69(100), 55, 41. Data are consistent with those obtained from the analysis of a commercially available sample.

1-tert-Butylcyclohexanol. GC–MS m/z (relative abundance): 156 (M<sup>+</sup>), 125, 123, 111, 99 (100), 81, 67, 57. Data are consistent with those obtained from the analysis of an authentic sample that was present in our laboratory from previous studies.<sup>40</sup>

2-tert-Butylcyclohexanone. GC-MS m/z (relative abundance): 154 (M<sup>+</sup>), 139, 110, 98 (100), 95, 83, 70, 57, 39. Spectrometric data are consistent with those reported in the literature.<sup>54</sup>

3-tert-Butylcyclohexanone. GC-MS m/z (relative abundance): 154 (M<sup>+</sup>), 98, 83, 81, 70, 69, 67, 57 (100). Data are consistent with those reported in the literature.<sup>55</sup>

4-tert-Butylcyclohexanone. GC-MS m/z (relative abundance): 154 (M<sup>+</sup>), 99, 98, 97, 83, 70, 69, 57 (100). Data are consistent with those obtained from the analysis of a commercially available sample.

1-Phenylcyclohexanol. GC-MS m/z (relative abundance): 176 (M<sup>+</sup>), 158, 143, 133, 120, 115, 105, 91, 77, 55 (100). Data are consistent with those obtained from the analysis of an authentic sample that was present in our laboratory from previous studies.<sup>40</sup>

2-Phenylcyclohexanone. GC-MS m/z (relative abundance): 174 (M<sup>+</sup>), 130 (100), 129, 115, 98, 83, 78, 70, 55. Data are consistent with those reported in the literature.<sup>50</sup>

*3-Phenylcyclohexanone.* GC–MS m/z (relative abundance): 174 (M<sup>+</sup>, 100), 145, 131, 117, 105, 91, 83, 70, 41. Data are consistent with those reported in the literature. <sup>56</sup>

*4-Phenylcyclohexanone.* GC–MS m/z (relative abundance): 174 (M<sup>+</sup>), 145, 130, 117, 104 (100), 91, 87, 65, 55. Data are consistent with those obtained from the analysis of a commercially available sample.

#### ASSOCIATED CONTENT

## **Solution** Supporting Information

The Supporting Information is available free of charge at https://pubs.acs.org/doi/10.1021/acs.joc.1c00902.

Analytical data, kinetic plots of  $k_{\text{obs}}$  vs substrate concentration for the reactions of the cycloalkanes with CumO $^{\bullet}$ ; computational details (PDF)

## AUTHOR INFORMATION

## **Corresponding Authors**

Fengjiao Liu — College of Chemistry and Chemical Engineering, Shanghai University of Engineering Science, Shanghai 201620, China; Department of Chemistry and Biochemistry, University of California, Los Angeles, California 90095, United States; Email: fjliu208@163.com

K. N. Houk — Department of Chemistry and Biochemistry, University of California, Los Angeles, California 90095, United States; orcid.org/0000-0002-8387-5261; Email: houk@chem.ucla.edu

Massimo Bietti – Dipartimento di Scienze e Tecnologie Chimiche, Università "Tor Vergata", I-00133 Rome, Italy; o orcid.org/0000-0001-5880-7614; Email: bietti@ uniroma2.it

#### **Authors**

Teo Martin — Dipartimento di Scienze e Tecnologie Chimiche, Università "Tor Vergata", I-00133 Rome, Italy; orcid.org/0000-0003-4584-4322

Marco Galeotti — Dipartimento di Scienze e Tecnologie Chimiche, Università "Tor Vergata", I-00133 Rome, Italy Michela Salamone — Dipartimento di Scienze e Tecnologie Chimiche, Università "Tor Vergata", I-00133 Rome, Italy; orcid.org/0000-0003-3501-3496

Yanmin Yu — Beijing Key Laboratory for Green Catalysis and Separation, Department of Environmental Chemical Engineering, Beijing University of Technology, Beijing 100124, China; Department of Chemistry and Biochemistry, University of California, Los Angeles, California 90095, United States; ⊚ orcid.org/0000-0002-4219-4611

Meng Duan – Department of Chemistry and Biochemistry, University of California, Los Angeles, California 90095, United States

Complete contact information is available at: https://pubs.acs.org/10.1021/acs.joc.1c00902

#### **Author Contributions**

<sup>⊥</sup>T.M. and M.G. contributed equally.

#### **Notes**

The authors declare no competing financial interest.

#### ACKNOWLEDGMENTS

We are grateful to the National Science Foundation (CHE-1764328), the University of Rome "Tor Vergata" (Project E84I20000250005), and the Shanghai Sailing Program (No. 20YF1416000) for financial support of this research. M.B. also thanks Miquel Costas for helpful discussions and Scott J. Miller for details on the synthesis of *tert*-butylcyclopentane.

## REFERENCES

(1) Cernak, T.; Dykstra, K. D.; Tyagarajan, S.; Vachal, P.; Krska, S. W. The Medicinal Chemist's Toolbox for Late Stage Functionalization of Drug-Like Molecules. *Chem. Soc. Rev.* **2016**, *45*, 546–576.

(2) (a) Davies, H. M. L.; Liao, K. Dirhodium Tetracarboxylates as Catalysts for Selective Intermolecular C-H Functionalization. *Nature Rev. Chem.* 2019, 3, 347–360. (b) Li, J.; Zhang, Z.; Wu, L.; Zhang, W.; Chen, P.; Lin, Z.; Liu, G. Site-specific allylic C-H bond functionalization with a copper-bound N-centred radical. *Nature* 2019, 574, 516–521. (c) White, M. C.; Zhao, J. Aliphatic C-H Oxidations for Late-Stage Functionalization. *J. Am. Chem. Soc.* 2018, 140, 13988–14009. (d) Hartwig, J. F. Evolution of C-H Bond Functionalization from Methane to Methodology. *J. Am. Chem. Soc.* 2016, 138, 2–24. (e) Yamaguchi, J.; Yamaguchi, A. D.; Itami, K. C-H Bond Functionalization: Emerging Synthetic Tools for Natural Products and Pharmaceuticals. *Angew. Chem., Int. Ed.* 2012, 51, 8960–9009. (f) Newhouse, T.; Baran, P. S. If C-H Bonds Could Talk: Selective C-H Bond Oxidation. *Angew. Chem., Int. Ed.* 2011, 50, 3362–3374.

(3) (a) Wein, L. A.; Wurst, K.; Angyal, P.; Weisheit, L.; Magauer, T. Synthesis of (—)-Mitrephorone A via a Bioinspired Late Stage C—H Oxidation of (—)-Mitrephorone B. J. Am. Chem. Soc. 2019, 141, 19589—19593. (b) Hung, K.; Condakes, M. L.; Novaes, L. F. T.; Harwood, S. J.; Morikawa, T.; Yang, Z.; Maimone, T. J. Development of a Terpene Feedstock-Based Oxidative Synthetic Approach to the Illicium Sesquiterpenes. J. Am. Chem. Soc. 2019, 141, 3083—3099. (c) Michaudel, Q.; Journot, G.; Regueiro-Ren, A.; Goswami, A.; Guo, Z.; Tully, T. P.; Zou, L.; Ramabhadran, R. O.; Houk, K. N.; Baran, P.

- S. Improving Physical Properties via C-H Oxidation: Chemical and Enzymatic Approaches. *Angew. Chem., Int. Ed.* **2014**, 53, 12091–12096.
- (4) (a) Kawamata, Y.; Yan, M.; Liu, Z.; Bao, D.-H.; Chen, J.; Starr, J. T.; Baran, P. S. Scalable, Electrochemical Oxidation of Unactivated C–H Bonds. J. Am. Chem. Soc. 2017, 139, 7448–7451. (b) Quinn, R. K.; Könst, Z. A.; Michalak, S. E.; Schmidt, Y.; Szklarski, A. R.; Flores, A. R.; Nam, S.; Horne, D. A.; Vanderwal, C. D.; Alexanian, E. J. Site-Selective Aliphatic C–H Chlorination Using N-Chloroamides Enables a Synthesis of Chlorolissoclimide. J. Am. Chem. Soc. 2016, 138, 696–702. (c) Liu, W.; Groves, J. T. Manganese Porphyrins Catalyze Selective C–H Bond Halogenations. J. Am. Chem. Soc. 2010, 132, 12847–12849.
- (5) Armanino, N.; Charpentier, J.; Flachsmann, F.; Goeke, A.; Liniger, M.; Kraft, P. What's Hot, What's Not: The Trends of the Past 20 Years in the Chemistry of Odorants. *Angew. Chem., Int. Ed.* **2020**, 59, 16310–16344.
- (6) Moteki, S. A.; Usui, A.; Zhang, T.; Solorio Alvarado, C. R.; Maruoka, K. Site-Selective Oxidation of Unactivated C-H Bonds with Hypervalent Iodine(III) Reagents. *Angew. Chem., Int. Ed.* **2013**, *52*, 8657–8660.
- (7) (a) Ravelli, D.; Fagnoni, M.; Fukuyama, T.; Nishikawa, T.; Ryu, I. Site-Selective C—H Functionalization by Decatungstate Anion Photocatalysis: Synergistic Control by Polar and Steric Effects Expands the Reaction Scope. ACS Catal. 2018, 8, 701–713. (b) Ni, L.; Ni, J.; Lv, Y.; Yang, P.; Cao, Y. Photooxygenation of Hydrocarbons over Efficient and Reusable Decatungstate Heterogenized on Hydrophobically-Modified Mesoporous Silica. Chem. Commun. 2009, 2171–2173.
- (8) England, P. A.; Rouch, D. A.; Westlake, A. C. G.; Bell, S. G.; Nickerson, D. P.; Webberley, M.; Flitsch, S. L.; Wong, L.-L. Aliphatic vs. Aromatic C–H Bond Activation of Phenylcyclohexane Catalysed by Cytochrome P450cam. *Chem. Commun.* 1996, 357–358.
- (9) (a) Milan, M.; Bietti, M.; Costas, M. Highly Enantioselective Oxidation of Nonactivated Aliphatic C–H Bonds with Hydrogen Peroxide Catalyzed by Manganese Complexes. ACS Cent. Sci. 2017, 3, 196–204. (b) Shen, D.; Miao, C.; Wang, S.; Xia, C.; Sun, W. Efficient Benzylic and Aliphatic C–H Oxidation with Selectivity for Methylenic Sites Catalyzed by a Bioinspired Manganese Complex. Org. Lett. 2014, 16, 1108–1111. (c) Zhang, Q.; Gorden, J. D.; Goldsmith, C. R. C–H Oxidation by H<sub>2</sub>O<sub>2</sub> and O<sub>2</sub> Catalyzed by a Non-Heme Iron Complex with a Sterically Encumbered Tetradentate N-Donor Ligand. Inorg. Chem. 2013, 52, 13546–13554. (d) Chen, M. S.; White, M. C. Combined Effects on Selectivity in Fe-Catalyzed Methylene Oxidation. Science 2010, 327, 566–571.
- (10) González-Núñez, M. E.; Castellano, G.; Andreu, C.; Royo, J.; Báguena, M.; Mello, R.; Asensio, G. Influence of Remote Substituents on the Equatorial/Axial Selectivity in the Monooxygenation of Methylene C–H Bonds of Substituted Cyclohexanes. *J. Am. Chem. Soc.* **2001**, *123*, 7487–7491.
- (11) Fu, J.; Ren, Z.; Bacsa, J.; Musaev, D. G.; Davies, H. M. L. Desymmetrization of Cyclohexanes by Site- and Stereoselective C–H Functionalization. *Nature* **2018**, *564*, 395–400.
- (12) Rodríguez, M.; Font, G.; Nadal-Moradell, J.; Hernán-Gómez, A.; Costas, M. Iron-Catalyzed Intermolecular Functionalization of Non-Activated Aliphatic C–H Bonds via Carbene Transfer. *Adv. Synth. Catal.* **2020**, *362*, 5116–5123.
- (13) (a) Niu, L.; Jiang, C.; Liang, Y.; Liu, D.; Bu, F.; Shi, R.; Chen, H.; Chowdhury, A. D.; Lei, A. Manganese-Catalyzed Oxidative Azidation of C(sp³)—H Bonds under Electrophotocatalytic Conditions. J. Am. Chem. Soc. 2020, 142, 17693—17702. (b) Margrey, K. A.; Czaplyski, W. L.; Nicewicz, D. A.; Alexanian, E. J. A General Strategy for Aliphatic C—H Functionalization Enabled by Organic Photoredox Catalysis. J. Am. Chem. Soc. 2018, 140, 4213—4217. (c) Sharma, A.; Hartwig, J. F. Metal-Catalysed Azidation of Tertiary C—H Bonds Suitable for Late-Stage Functionalization. Nature 2015, 517, 600—604.
- (14) (a) Amaoka, Y.; Kamijo, S.; Hoshikawa, T.; Inoue, M. Radical Amination of  $C(sp^3)$ -H Bonds Using N-Hydroxyphthalimide and

- Dialkyl Azodicarboxylate. *J. Org. Chem.* **2012**, 77, 9959–9969. (b) Melone, L.; Gambarotti, C.; Prosperini, S.; Pastori, N.; Recupero, F.; Punta, C. Hydroperoxidation of Tertiary Alkylaromatics Catalyzed by *N*-Hydroxyphthalimide and Aldehydes under Mild Conditions. *Adv. Synth. Catal.* **2011**, 353, 147–154. (c) Arends, I. W. C. E.; Sasidharan, M.; Kühnle, A.; Duda, M.; Jost, C.; Sheldon, R. A. Selective Catalytic Oxidation of Cyclohexylbenzene to Cyclohexylbenzene-1-Hydroperoxide: a Coproduct-Free Route to Phenol. *Tetrahedron* **2002**, 58, 9055–9061.
- (15) (a) Herron, A. N.; Liu, D.; Xia, G.; Yu, J.-Q. δ-C-H Monoand Dihalogenation of Alcohols. J. Am. Chem. Soc. 2020, 142, 2766-2770. (b) Andrä, M. S.; Schifferer, L.; Pollok, C. H.; Merten, C.; Gooßen, L. J.; Yu, J.-Q. Enantio- and Diastereoswitchable C-H Arylation of Methylene Groups in Cycloalkanes. Chem. - Eur. J. 2019, 25, 8503-8507. (c) Wu, S.; Wu, X.; Wang, D.; Zhu, C. Regioselective Vinylation of Remote Unactivated  $C(sp^3)$ -H Bonds: Access to Complex Fluoroalkylated Alkenes. Angew. Chem., Int. Ed. 2019, 58, 1499-1503. (d) Chen, H.; Guo, L.; Yu, S. Primary, Secondary, and Tertiary γ-C(sp<sup>3</sup>)-H Vinylation of Amides via Organic Photoredox-Catalyzed Hydrogen Atom Transfer. Org. Lett. 2018, 20, 6255-6259. (e) Kim, I.; Park, B.; Kang, G.; Kim, J.; Jung, H.; Lee, H.; Baik, M.-H.; Hong, S. Visible-Light-Induced Pyridylation of Remote  $C(sp^3)$ -H Bonds by Radical Translocation of N-Alkoxypyridinium Salts. Angew. Chem., Int. Ed. 2018, 57, 15517-15522. (f) Shu, W.; Lorente, A.; Gómez-Bengoa, E.; Nevado, C. Expeditious diastereoselective synthesis of elaborated ketones via remote Csp3-H functionalization. Nat. Commun. 2017, 8, 13832. (g) Wasa, M.; Chan, K. S. L.; Zhang, X.-G.; He, J.; Miura, M.; Yu, J.-Q. Ligand-Enabled Methylene  $C(sp^3)$ -H Bond Activation with a Pd(II) Catalyst. J. Am. Chem. Soc. **2012**, 134, 18570-18572.
- (16) Salamone, M.; Ortega, V. B.; Bietti, M. Enhanced Reactivity in Hydrogen Atom Transfer from Tertiary Sites of Cyclohexanes and Decalins via Strain Release. Equatorial C—H Activation vs Axial C—H Deactivation. *J. Org. Chem.* **2015**, *80*, 4710–4715.
- (17) Salamone, M.; Bietti, M. Reaction Pathways of Alkoxyl Radicals. The Role of Solvent Effects on C–C Bond Fragmentation and Hydrogen Atom Transfer Reactions. *Synlett* **2014**, *25*, 1803–1816
- (18) Bietti, M.; Martella, R.; Salamone, M. Understanding Kinetic Solvent Effects on Hydrogen Abstraction Reactions from Carbon by the Cumyloxyl Radical. *Org. Lett.* **2011**, *13*, 6110–6113.
- (19) Salamone, M.; Martin, T.; Milan, M.; Costas, M.; Bietti, M. Electronic and Torsional Effects on Hydrogen Atom Transfer from Aliphatic C–H Bonds. A Kinetic Evaluation via Reaction with the Cumyloxyl Radical. *J. Org. Chem.* **2017**, *82*, 13542–13549.
- (20) The *cis-trans* stereoselectivity has been previously investigated in C–H bond hydroxylations at C-3 and C-4 of methylcyclohexane and *tert*-butylcyclohexane promoted by TFDO (ref 10) and of *tert*-butylcyclohexane with  $H_2O_2$  catalyzed by the  $Mn(^{TIPS}mcp)$  complex (ref 21).
- (21) Dantignana, V.; Milan, M.; Cussó, O.; Company, A.; Bietti, M.; Costas, M. Chemoselective Aliphatic C–H Bond Oxidation Enabled by Polarity Reversal. *ACS Cent. Sci.* **2017**, *3*, 1350–1358.
- (22) SPARTAN'18; Wavefunction, Inc., Irvine, CA, 2018.
- (23) Stewart, J. J. P. Optimization of Parameters for Semiempirical Methods V: Modification of NDDO Approximations and Application to 70 Elements. *J. Mol. Model.* **2007**, *13*, 1173–1213.
- (24) Chai, J. D.; Head-Gordon, M. Long-range corrected hybrid density functionals with damped atom-atom dispersion corrections. *Phys. Chem. Chem. Phys.* **2008**, *10*, 6615–6620.
- (25) Cossi, M.; Barone, V.; Mennucci, B.; Tomasi, J. Ab initio study of ionic solutions by a polarizable continuum dielectric model. *Chem. Phys. Lett.* **1998**, 286, 253–260.
- (26) Frisch, M. J.; Trucks, G. W.; Schlegel, H. B.; Scuseria, G. E.; Robb, M. A.; Cheeseman, J. R.; Scalmani, G.; Barone, V.; Petersson, G. A.; Nakatsuji, H.; Li, X.; Caricato, M.; Marenich, A. V.; Bloino, J.; Janesko, B. G.; Gomperts, R.; Mennucci, B.; Hratchian, H. P.; Ortiz, J. V.; Izmaylov, A. F.; Sonnenberg, J. L.; Williams-Young, D.; Ding, F.; Lipparini, F.; Egidi, F.; Goings, J.; Peng, B.; Petrone, A.; Henderson,

- T.; Ranasinghe, D.; Zakrzewski, V. G.; Gao, J.; Rega, N.; Zheng, G.; Liang, W.; Hada, M.; Ehara, M.; Toyota, K.; Fukuda, R.; Hasegawa, J.; Ishida, M.; Nakajima, T.; Honda, Y.; Kitao, O.; Nakai, H.; Vreven, T.; Throssell, K.; Montgomery, J. A., Jr.; Peralta, J. E.; Ogliaro, F.; Bearpark, M. J.; Heyd, J. J.; Brothers, E. N.; Kudin, K. N.; Staroverov, V. N.; Keith, T. A.; Kobayashi, R.; Normand, J.; Raghavachari, K.; Rendell, A. P.; Burant, J. C.; Iyengar, S. S.; Tomasi, J.; Cossi, M.; Millam, J. M.; Klene, M.; Adamo, C.; Cammi, R.; Ochterski, J. W.; Martin, R. L.; Morokuma, K.; Farkas, O.; Foresman, J. B.; Fox, D. J. Gaussian, Inc., Wallingford, CT, 2016.
- (27) Zou, L.; Paton, R. S.; Eschenmoser, A.; Newhouse, T. R.; Baran, P. S.; Houk, K. N. Enhanced Reactivity in Dioxirane C-H Oxidations via Strain Release: A Computational and Experimental Study. *J. Org. Chem.* **2013**, *78*, 4037–4048.
- (28) Yang, Z.; Yu, P.; Houk, K. N. Molecular Dynamics of Dimethyldioxirane C–H Oxidation. *J. Am. Chem. Soc.* **2016**, *138*, 4237–4242.
- (29) Shuler, W. G.; Johnson, S. L.; Hilinski, M. K. Organocatalytic, Dioxirane-Mediated C–H Hydroxylation under Mild Conditions Using Oxone. *Org. Lett.* **2017**, *19*, 4790–4793.
- (30) Salamone, M.; Bietti, M. Unpublished results.
- (31) Mello, R.; Fiorentino, M.; Fusco, C.; Curci, R. Oxidations by Methyl(trifluoromethyl)dioxirane. 2. Oxyfunctionalization of Saturated Hydrocarbons. *J. Am. Chem. Soc.* **1989**, *111*, 6749–6757.
- (32) Wang, Y.; Hu, X.; Morales-Rivera, C. A.; Li, G.-X.; Huang, X.; He, G.; Liu, P.; Chen, G. Epimerization of Tertiary Carbon Centers via Reversible Radical Cleavage of Unactivated C(sp³)-H Bonds. J. Am. Chem. Soc. 2018, 140, 9678–9684.
- (33) Annunziatini, C.; Gerini, M. F.; Lanzalunga, O.; Lucarini, M. Aerobic Oxidation of Benzyl Alcohols Catalyzed by Aryl Substituted *N*-Hydroxyphthalimides. Possible Involvement of a Charge-Transfer Complex. *J. Org. Chem.* **2004**, *69*, 3431–3438.
- (34) Eisenbraun, E. J. Cyclooctanone. Org. Synth. 1973, 5, 310-312.
- (35) Kim, B.; Chinn, A. J.; Fandrick, D. R.; Senanayake, C. H.; Singer, R. A.; Miller, S. J. Distal Stereocontrol Using Guanidinylated Peptides as Multifunctional Ligands: Desymmetrization of Diarylmethanes via Ullman Cross-Coupling. *J. Am. Chem. Soc.* **2016**, *138*, 7939–7945.
- (36) (a) Pines, H.; Ipatieff, V. N. Synthesis of *t*-Butyl- and *t*-Amylcyclopentane and of their Intermediate Products. *J. Am. Chem. Soc.* **1939**, *61*, 2728–2730. (b) Anet, F. A. L.; St. Jacques, M.; Chmurny, G. N. Restricted rotation in *tert*-butylcycloalkanes. Effect of ring size. *J. Am. Chem. Soc.* **1968**, *90*, 5243–5246.
- (37) Ramazanov, I. R.; Sharipova, A. Z.; Dzhemilev, U. M. Cp<sub>2</sub>TiCl<sub>2</sub>-catalyzed hydroalkylation of cycloalkenes with *t*-BuBr-Et<sub>3</sub>Al. *Russ. J. Org. Chem.* **2006**, *42*, 1858–1860.
- (38) Beard, C. D.; Baum, K.; Grakauskas, V. Synthesis of some novel trifluoromethanesulfonates and their reactions with alcohols. *J. Org. Chem.* **1973**, 38, 3673–3677.
- (39) Hartmann, R. W.; Batzl, C. Synthesis and evaluation of 4-alkylanilines as mammary tumor inhibiting aromatase inhibitors. *Eur. J. Med. Chem.* **1992**, *27*, 537–544.
- (40) Aureliano Antunes, C. S.; Bietti, M.; Lanzalunga, O.; Salamone, M. Photolysis of 1-Alkylcycloalkanols in the Presence of (Diacetoxyiodo)benzene and  $I_2$ . Intramolecular Selectivity in the  $\beta$ -Scission Reactions of the Intermediate 1-Alkylcycloalkoxyl Radicals. *J. Org. Chem.* **2004**, *69*, 5281–5289.
- (41) Fisher, R. D.; Bogard, T. D.; Kovacic, P. Chemistry of n-haloamines. XVIII. Rearrangement of 1-N,N-dichloroaminoapocamphane by aluminum chloride. *J. Am. Chem. Soc.* **1973**, *95*, 3646–3651.
- (42) Abdelshafeek, K. A.; Elgendy, H. A.; ElMissiry, M. M.; Seif ElNasr, M. M. Isolation and identification of some chemical constituents and antimicrobial activity of two Lamiaceae plants growing in Saini. *Egypt. J. Chem.* **2016**, *59*, 21–31.
- (43) Plietker, B.; Niggermann, M.; Pollrich, A. The acid accelerated ruthenium-catalysed dihydroxylation. Scope and limitations. *Org. Biomol. Chem.* **2004**, *2*, 1116–1124.

- (44) Guthrie, J. P.; Guo, J. Intramolecular Aldol Condensations: Rate and Equilibrium Constants. *J. Am. Chem. Soc.* **1996**, *118*, 11472—11487.
- (45) Andrew, D.; Weedon, A. C. Determination of the Relative Rates of Formation, Fates, and Structures of Triplet 1,4-Biradicals Generated in the Photochemical Cycloaddition Reactions of 2-Cyclopentenones with 2-Methylpropene. *J. Am. Chem. Soc.* **1995**, *117*, 5647–5663.
- (46) Suzuki, M.; Suzuki, T.; Kawagishi, T.; Morita, Y.; Noyori, R. Conjugate Addition of Phosphine-Complexed Organocopper Reagents to α,β-Unsaturated Ketones. *Isr. I. Chem.* **1984**, 24, 118–124.
- (47) Molander, G. A.; McKie, J. A. Intramolecular nucleophilic acyl substitution reactions of halo-substituted esters and lactones. New applications of organosamarium reagents. *J. Org. Chem.* **1993**, *58*, 7216–7227.
- (48) Streuff, J.; Feurer, M.; Bichovski, P.; Frey, G.; Gellrich, U. Enantioselective Titanium(III)-Catalyzed Reductive Cyclization of Ketonitriles. *Angew. Chem., Int. Ed.* **2012**, *51*, 8661–8664.
- (49) Zhou, L.; Zhang, Y.; Shi, D. Samarium(II) Iodide-Promoted Intermolecular and Intramolecular Ketone-Nitrile Reductive Coupling Reactions. *Synthesis* **2000**, 2000, 91–98.
- (50) Pecunioso, A.; Menicagli, R. Efficient conjugate alkylation of alpha, beta-unsaturated nitro olefins by triorganoalanes. *J. Org. Chem.* **1988**, *53*, 45–49.
- (51) Mubarak, M. S.; Pagel, M.; Marcus, L. M.; Peters, D. G. Formation of 2-(3'-Oxocyclohexyl)-2-cyclohexen-1-one via Reduction of 2-Cyclohexen-1-one with Electrogenerated Nickel(I) Salen. *J. Org. Chem.* **1998**, 63, 1319–1322.
- (52) Wei, Y.; Rao, B.; Cong, X.; Zeng, X. Highly Selective Hydrogenation of Aromatic Ketones and Phenols Enabled by Cyclic (Amino)(alkyl)carbene Rhodium Complexes. *J. Am. Chem. Soc.* **2015**, 137, 9250–9253.
- (53) Russell, G. A.; Baik, W.; Ngoviwatchai, P.; Kim, B. H. Electron Transfer Processes. Part 47. Reactions of Organometallic Reagents Involving Electron Transfer. *Acta Chem. Scand.* **1990**, 44, 170–177.
- (54) House, H. O.; Outcalt, R. J.; Cliffton, M. D. Enones with strained double bonds. 7. Precursors for substituted bicyclo[3.3.1]-nonane systems. *J. Org. Chem.* **1982**, *47*, 2413–2419.
- (55) Kamata, K.; Yonehara, K.; Nakagawa, Y.; Uehara, K.; Mizuno, N. Efficient stereo- and regioselective hydroxylation of alkanes catalysed by a bulky polyoxometalate. *Nat. Chem.* **2010**, *2*, 478–483. (56) Bedford, R. B.; Betham, M.; Charmant, J. P. H.; Haddow, M. F.; Guy Orpen, A.; Pilarski, L. T.; Coles, S. J.; Hursthouse, M. B.

Simple Palladacyclic and Platinacyclic Catalysts for the 1,4-Conjugate

Addition of Arylboronic Acids and Arylsiloxanes to Enones. *Organometallics* **2007**, *26*, 6346–6353.